17th World Conference on Earthquake Engineering, 17WCEE
Sendai, Japan - September 13th to 18th 2020

INVESTIGATION OF THE SHORT-PERIOD PARADOX FOR STEEL SPECIAL CONCENTRICALLY BRACED FRAME BUILDINGS

S. Wichman[(1)], J. Berman[(2)], D. Lehman[(3)], G. Kingsley[(4)]

[(1)] *Graduate Research Assistant, University of Washington, wichman@uw.edu*
[(2)] *Professor, University of Washington, jwberman@uw.edu*
[(3)] *Professor, University of Washington, delehman@uw.edu*
[(4)] *President and CEO, KL&A Engineers & Builders, Golden, CO, gkingsley@klaa.com*

Abstract

Most buildings in the United States are low-rise, commercial, and multi-family dwelling buildings with a short fundamental period. These buildings are designed in accordance with ASCE/SEI 7-16, Minimum Design Loads for Buildings and Other Structures, which is adopted by reference in the International Building Code. These codes are intended to achieve a uniform seismic risk for all buildings designed using the code, however, nonlinear dynamic analysis results have shown that short period buildings designed in accordance to the code actually have a higher calculated risk of collapse than the collapse probability target of ASCE/SEI 7-16. Observed earthquake damage of short period buildings from recent major earthquakes do not confirm this higher calculated risk of collapse from the nonlinear dynamic analysis, raising questions and indicating a lack of validation for the current analysis and modeling techniques for short period buildings.

This disagreement is often referred to as the short period building paradox and is currently being investigated by the Applied Technology Council (ATC), which was commissioned by the Federal Emergency Management Agency (FEMA) under the ATC-116 Project, Solutions to the Issue of Short Period Building Performance. Here, results of nonlinear dynamic analyses of short period Steel Concentrically Braced Frame buildings, conducted using the methodology of FEMA P-695, *Quantification of Building Seismic Performance Factors,* as part of the ATC-116 Project will be presented. A three-dimensional numerical model in OpenSees was created and includes many factors to determine what could contribute to the paradox and discrepancy between analysis results and observations. Results show that using a more sophisticated model that includes the contribution of the gravity frame, moment frame action within the braced frame, and deteriorating connection models results in a collapse probability that decreases with decreasing fundamental period. Results also show that when modeling the contribution of soil structure interaction and foundation flexibility, braces will rock on their foundations, resulting in less strength and more ductility. Ultimately, results show that the use of improved nonlinear dynamic numerical models can begin to explain the paradox, brining numerical results into closer alignment with observed collapse records.

Keywords: Steel, Special Concentrically Braced Frames, Collapse Probability, Short Period Paradox

1. Introduction & Background

Given risk-targeted maximum considered earthquake (MCE_R) ground motions, Risk Category II buildings designed in accordance with ASCE/SEI 7-10 are expected to not exceed a collapse probability of 10 percent. Studies that use the collapse probability methodology described in FEMA P-695, *Quantification of Building Seismic Performance Factors* [1], such as those found in NIST [2] found that most buildings with a period greater than 0.5 seconds, achieved the intended seismic performance target. However, for buildings with periods less than 0.5 seconds (short period buildings), the probability of collapse actually increased with decreasing period, and in some cases exceeded the 10 percent probability of collapse given MCE_R ground motions. The increase in collapse probability for short period buildings is a trend that has not been reflected in actual earthquake damage such as that observed in the 1994 Northridge earthquake. Field observations after this earthquake suggested that damage to these buildings was limited and did not cause collapse. This suggests that in the past, numerical models have overestimated the collapse risk of short-period buildings. This observation has been called the "short period paradox".

Although this paradox has been observed across many different seismic-force-resisting systems and construction materials, this paper will focus on the conclusions from a study on the collapse probability of steel special concentrically braced frames (SCBFs) using the P-695 analysis. The study attempts to develop improved numerical models for steel SCBFs that more accurately predict collapse in a way that is consistent with post-earthquake observations. For this study, practicing engineers designed the archetype buildings used for the analysis. These archetypes are all designed according to current American Institute of Steel Construction (AISC) specifications and are intended to broadly represent common steel braced frame building types and expected structural behaviors routinely encountered in practice.

2. Design of Special Concentrically Braced Frames

Concentric Braced Frames (CBF's) are composed of braces, gusset plates, beams, and columns. The centerlines of the braces, beams, and columns join at a single, concentric, or nearly concentric point. The braces are the primary source of lateral resistance, and are typically configured with opposing, paired braces. Special Concentric Braced Frames (SCBF's) are detailed in accordance with AISC provisions intended to encourage ductile response under cyclic loads. However, the seismic response of SCBF's also depends on the frame members and their connections. These members provide additional strength and stiffness that becomes particularly important after brace facture, whether or not the frame was designed to be moment resistant.

3. Building Archetypes and Designs

The building archetypes selected for this study were intended to represent code-compliant modern construction that adopt a steel structural system with lateral loads carried by SCBF's. The buildings broadly represent common steel braced frame building types and expected structural behaviors that are often found in practice; they are not intended to represent special or innovative designs. All archetypes were designed for commercial office occupancies as many steel SCBF buildings fit into this category, and all archetypes were designed to current American Institute of Steel Construction (AISC) specifications.

This paper looks at ten different archetypes of short-period SCBF's that considered a range of potential parameters in building design and analysis that may affect the collapse probability. Specifically, variations in the archetypes include: (1) number of stories; (2) level of seismicity; and (3) soil structure interaction (SSI) and foundation flexibility. Table 1 summarizes the ten different archetypes and their properties. The baseline archetypes are the six archetypes that include variations in three building heights and two levels of seismicity that do not consider the effects of SSI and foundation flexibility. The remaining archetypes are variations of the two- and four-story high-seismic baseline archetypes for a SSI and

foundation flexibility parametric study. For this parametric study, soft soil properties and stiff soil properties were both considered.

Table 1 – Summary of building archetypes analyzed in this study

Parametric Study	Archetype ID	No. of Stories	Level of Seismicity	SSI
Baseline	COM1B	1	High	N/A
	COM2B	2	High	N/A
	COM3B	4	High	N/A
	COM4B	1	Very high	N/A
	COM5B	2	Very high	N/A
	COM6B	4	Very high	N/A
Soil Structure Interaction and Foundation Flexibility	COM2B-SS1	2	High	Stiff
	COM2B-SS2	2	High	Soft
	COM3B-SS1	4	High	Stiff
	COM3B-SS2	4	High	Soft

3.1 Baseline Configurations

Two levels of seismicity, “high seismic” and “very high seismic”, were considered for the archetypes. The high seismic demand is located where MCE_R ground motions are characterized by a mapped short-period response acceleration S_S of 1.5g and corresponds to Seismic Design Category (SDC) D in the 2015 IBC and ASCE/SEI 7-10. The very high seismic level was intended to capture more severe seismic hazard levels, such as those located close to a fault. The archetype designs were prepared for 150% of the basic value, corresponding to SDC E. Table 2 shows a summary of the seismic loads used for the design.

Table 2 – Seismic loads used for design

Seismic Design Category	MCE_R Ground Motion Definition				
	S_1 (g)	S_S (g)	F_a	S_{MS} (g)	S_{DS} (g)
SDC D	0.60	1.50	1.0	1.50	1.0
SDC E	0.90	2.25	1.0	2.25	1.5

All archetypes had a 90-foot x 180-foot rectangular plan with grid spacing of 30-foot x 30-foot, as seen in Figure 1. In elevation, the baseline archetypes were either one-, two-, or four-stories with 14-foot story heights. The seismic-force-resisting systems consisted of two braced bays on each exterior face of the building. The braces occupied the entire 30-foot bays and were continuous from the roof to the foundation. The baseline brace configurations for the two- and four-story buildings were multi-story X configurations and the brace configuration for the one-story building was a chevron configuration. Although other grid spacing’s could also be representative of common commercial buildings, this configuration was selected to maintain bi-direction symmetry and to simplify the mathematical modeling. Figure 2 shows the isometric illustrated view of the COM2B archetype.

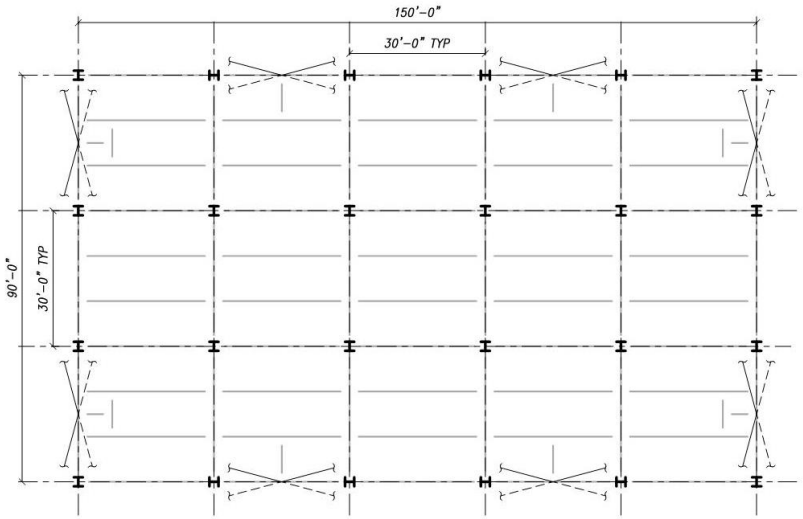

Figure 1 - Plan configuration for all baseline archetypes.

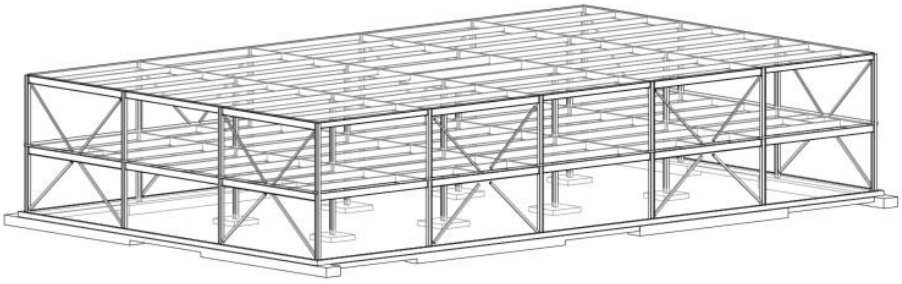

Figure 2 - Isometric view of the baseline archetype COM2B.

3.2 Soil-Structure Interaction and Foundation Flexibility Parametric Study

The influence of soil structure interaction and foundation flexibility on the behavior and collapse probability was studied by creating a variation of the baseline two-story and four-story high-seismic archetypes (COM2B and COM3B). For each of these two baseline configurations, the archetypes were modified from considering a rigid foundation and soil base to one that models either stiff soil (3000 psf allowable bearing pressure) and soft soil (1500 psf allowable bearing pressure).

The archetypes, which include SSI and foundation flexibility, have shallow spread-footing foundation with a slab-on-grade. The interior gravity columns sat on isolated spread footings, while the exterior braces were a continuous footing across the width of the braced frame. The footings sizes satisfy stability from overturning and allowable soil bearing pressures as required by the AISC code. These footing designs are intended to be representative of typical systems and are appropriate for studying the inclusion or exclusion of foundation flexibility in response prediction.

4. Braced Frame Modeling

The Archetypes in this study were all modeled in three dimensions using the nonlinear structural analysis program OpenSees [3]. Recent research on the nonlinear seismic response of SCBFs was drawn upon to develop the component behaviors used in these models.

4.1 Nonlinear Analysis Modeling Approach

Prior research on brace modeling methodology from Hsiao et al. [4, 5] and further extended by Sen et at. [6] was used to in this study to model the braces. The brace model consisted of displacement-based beam-column elements with distributed plasticity and a fiber cross section. The material model assigned to the brace fibers was a Giuffre-Menegotto-Pinto stress-strain model (Steel02 uniaxial material in OpenSees). A material wrapper, which uses the strain range of the fiber (i.e. the maximum range of strain from compression to tension in the fiber), simulated fracture of the brace. When the strain range in the fiber reached a Maximum Strain Range (MSR), defined by Equation (1), fracture of the fiber occurs and a near-zero value is assigned to the fiber stress and modulus.

$$MSR_f = 0.554(b/t)^{-0.75} (L_c/r)^{-0.47} (E/F_y)^{0.21} (\delta_{c,max}/\delta_{t,max})^{0.068} \quad (1)$$

In Equation (1), b/t is the local slenderness ratio and L_c/r is the global slenderness ratio, in which L_c is the effective length (KL) and r is the radius of gyration. In addition, E/F_y is the ratio between the modulus of elasticity and the brace yield stress used in the analysis (R_yF_y), and $\delta_{c,max}/\delta_{t,max}$ is the ratio between axial compression and tension deformation in the brace.

In the archetype design, braces connect to the beams and columns with gusset plates, which are configured to allow out-of-plane bucking of the braces under compression by forming a yield line near the end of the brace. Per recommendations in Hsaio et al. [4], the archetype models include out-of-plane rotational springs at the brace ends and a region of the beams and columns adjacent to the brace are rigid to capture this out-of-plane buckling behavior and to provide the best approximation of the actual behavior in terms of strength, stiffness, and post-buckling behavior.

Displacement-based beam-column elements with distributed plasticity and fiber-discretized cross sections modeled the beams located within the braced frames. Again, a Giuffre-Menegotto-Pinto model was used as the material model in the fibers. Because all beam designs meet seismic compactness requirements, the models neglect deterioration in the beam flexural and axial strengths. Elastic beam-column elements with discrete nonlinear rotational springs at each end represent the nonlinear behavior of the columns in both the strong and weak axis directions. The behavior of the rotational nonlinear springs is derived according to recommendations in NIST GCR 17-917-46v2, *Guidelines for Nonlinear Structural Analysis for Design of Buildings: Part IIa-Steel Moment Frames* [7] and Lignos et al. [8]. The component model used is the modified Ibarra-Madina-Krawinkler phenomenological component model, available in OpenSees.

All gravity frame members were included in the model to account for the contribution of the gravity frame to the overall system response. The gravity beams and columns were modeled using the same methods as the beams and columns located within the braced frame. Rigid diaphragm constraints and corotational element formulations were used in OpenSeens to account for nonlinear geometric effects. As recommended by FEMA P-695, the load combination 1.05D + 0.25L, where D and L are the dead and live loads respectively, was used to calculate both the gravity loads and seismic mass (assigned only in the horizontal displacement degrees of freedom) in the model.

4.2 Modeling Soil Structure Interaction and Foundation Flexibility

The effects of SSI and foundation flexibility were considered by simulating: (1) soil deformation; (2) foundation sliding; (3) foundation uplift and rotation; and (4) the impact of kinematic reduction in ground motion input. Figure 3 shows how each of the footings under the braced frames were discretized into eight beam-with-hinges elements. Also seen in Figure 3, springs and dampers at each of the nodes along the footings of the braced frames modeled the soil uplift and sliding. Under the isolated footings, a single spring and damper modeled the soil supporting the gravity columns.

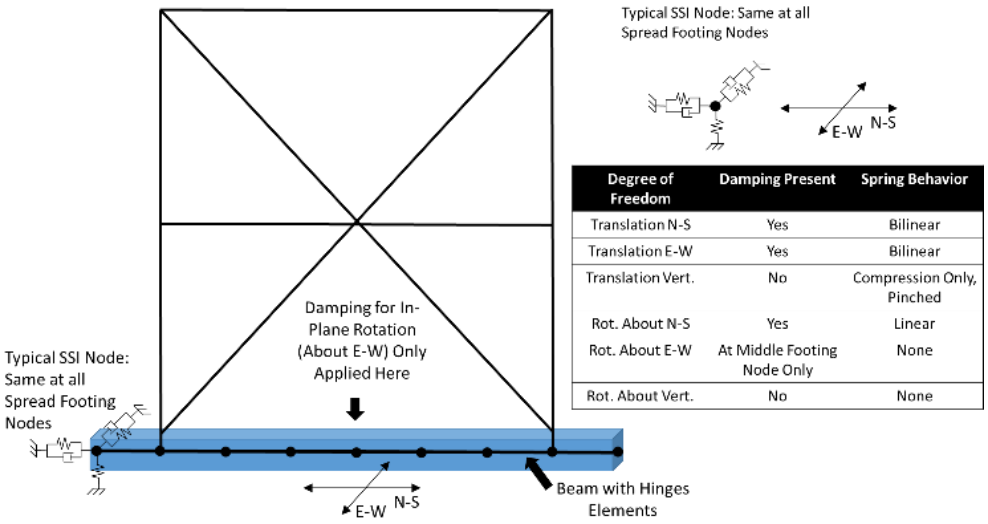

Figure 3 - Schematic of spread footing and SSI springs and dampers

5. Nonlinear 3D Seismic Analysis

5.1 Baseline Parametric Study

Nonlinear static pushover analyses were conducted on each of the baseline archetype models in each orthogonal direction to determine the overall backbone base shear verses roof drift response and to extract all needed data for the P-695 analyses. Results from the pushover analysis in one of the orthogonal directions, are shown in Figure 4; the response in the other direction was similar. Table 3 shows values of major parameters characterizing the normalized pushover curves. In the table, $V_{max,avg}$ is the average of the two maximum base shears developed in each of the orthogonal directions and $\Delta_{u,max}$ is the maximum roof drift ratio at collapse. Ω is the over-strength factor computed using the minimum lateral strength from the two orthogonal directions, per the P-695 methodology and μ_T is the period-based ductility computed per the P-695 methodology.

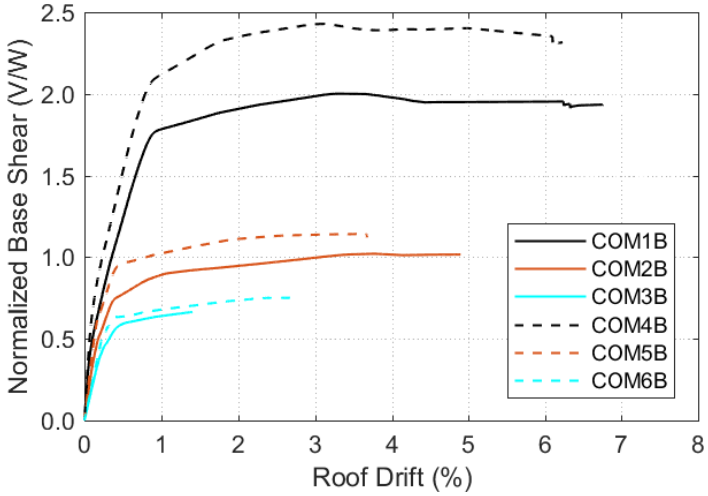

Figure 4 - Pushover curves for baseline models normalized by weight and roof height.

Table 3 – Static pushover results for baseline models

Archetype ID	No. of Stories	Level of Seismicity	T_{avg} (sec)	$V_{max,avg}$/ W	$\Delta_{u,max}$ (in/in)	Ω	μ_T
COM1B	1	High	0.17	1.92	0.07	11.0	14.0
COM2B	2	High	0.27	1.01	0.05	6.0	10.0
COM3B	4	High	0.47	0.66	0.02	3.9	3.15
COM4B	1	Very high	0.16	2.34	0.06	9.0	10.7
COM5B	2	Very high	0.25	1.10	0.04	4.2	6.8
COM6B	4	Very high	0.44	0.74	0.03	2.9	5.4

It is worth noting that the over-strength values, Ω, are very high. Although smaller over-strength values were intended in design, analysis values were much higher for three main reasons. First, a limited selection of brace sizes are available that meet seismic compactness requirements; when seismic demand is low in small buildings, a small change in brace size can result in a large change in capacity relative to demand. Second, the selection of braces sizes is based on compressive resistance of braces only; for smaller loads, slender braces are typically selected and the difference in compressive and tensile capacity can actually be quite large. Finally, the over-strength is also high because the contributions of the gravity frame and the moment frame action are not negligible; however, it is neglected in design. From Figure 4, it is also worth noting that the archetypes design for very high seismicity are not resulting in 50% additional strength. This is because the availability of brace sizes that meet slenderness requirements is limited, resulting in lower over-strength for the architypes designed for the very high levels of seismicity.

Incremental dynamic analysis (IDAs) were also conducted on all archetype models per the FEMA P-695 methodology using OpenSees. The typical sequence of yielding and failure modes was: (1) brace bucking; (2) brace yielding; (3) yielding of columns at their bases; (4) yielding of shear plate connections; (5) deterioration in strength of all yielded components; (6) brace fracture; and (7) sidesway collapse as the p-delta loads exceed the deteriorated column flexural strength and the deteriorated gravity frame and collector connection strengths. Figure 5 shows the results of the IDAs for the baseline archetypes. The points in Figure 5 represent the collapse fraction from the IDAs at each increment verses the S_T, the median spectral acceleration of the record set for that strip multiplied by the 3D analysis factor of 1.2. The figure also shows the smoothed collapse fragility curves which are anchored by S_{CT}, the median from the IDA curves, multiplied by the spectral shape factor in addition to the 3D factor. The fragility curves assume a β factor of 0.5.

Table 4 shows key values extracted from the IDA plots. The collapse margin ratio (CMR_{3D}) is computed as the ratio of $1.2S_{CT}$ to the MCE_R spectral acceleration used for design, S_{MT}. The probability of collapse for each of the baseline archetypes at the MCE_R spectral acceleration is computed using the smooth fragility curves shown in Figure 5. It is worth noting that the probability of collapse in the MCE_R ground motions is lower for the one- and two-story archetypes and the collapse probabilities are larger for archetypes design for the very high seismic demand. This is because the archetypes designed for the very high seismic demand had a lower over-strength, as discussed previously. In general, the probability of collapse decreases with increasing over-strength and increasing building height (and building period), and increasing building height is correlated with decreasing over-strength, so the collapse probability is shown to decrease with decreasing building height.

Table 4 – Collapse results for baseline models

Archetype ID	No. of Stories	Level of Seismicity	S_{MT} (g)	S_{CT} (g)	CMR_{3D}	$P[CO\|MCE_R]$

COM1B	1	High	1.5	2.90	2.32	1.2%
COM2B	2	High	1.5	2.34	1.87	3.4%
COM3B	4	High	1.5	2.29	1.83	6.0%
COM4B	1	Very high	2.25	3.31	1.77	4.0%
COM5B	2	Very high	2.25	2.13	1.14	20.4%
COM6B	4	Very high	2.25	2.27	1.21	18.6%

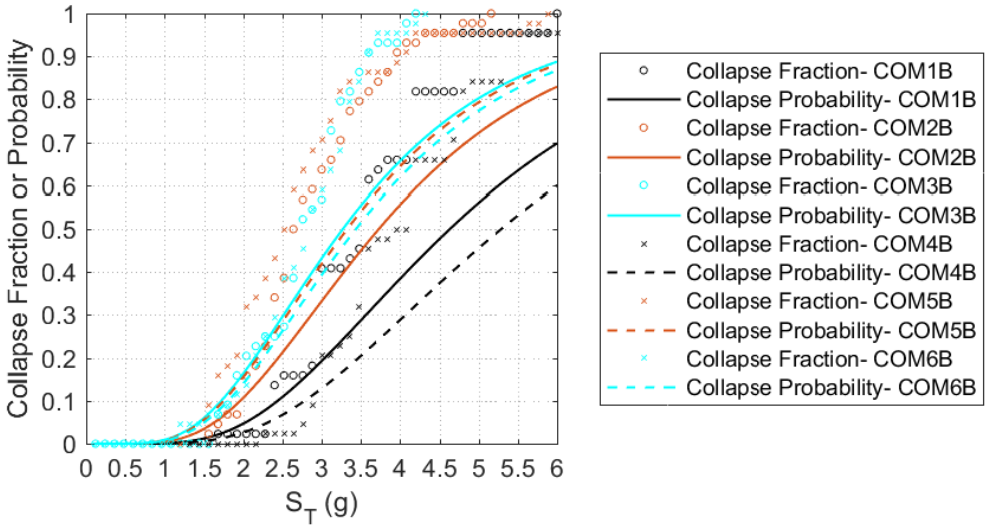

Figure 5 - Collapse fraction and collapse probability curves vs S_T from IDA analyses for the baseline models

5.2 Soil-Structure Interaction and Foundation Flexibility Parametric Study

Nonlinear static pushover analyses were also conducted for the archetypes considering SSI and foundation flexibility. Figure 6 shows results from the pushover analysis in one of the orthogonal directions; the response in each of the orthogonal directions was similar. Table 5 summarizes major parameters characterizing the normalized pushover curves. The first mode periods are much greater for the models with SSI, than for the baseline models, especially for the models with soft soil parameters. This is a result of soil flexibility and foundation sliding and overturning.

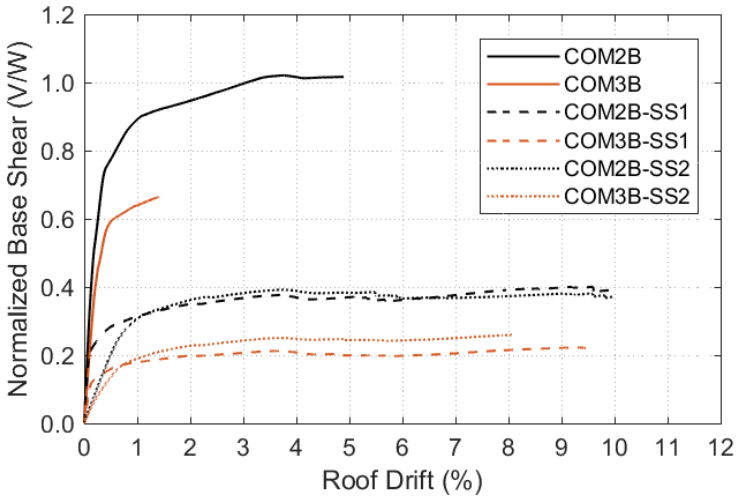

Figure 6 - Pushover curves for SSI archetype models normalized by weight and roof height.

Table 5 – Static pushover results for SSI archetype models

Archetype ID	No. of Stories	SSI	T_{avg} (sec)	$V_{max,avg}/W$	$\Delta_{u,max}$ (in/in)	Ω	μ_T
COM2B	2	N/A	0.27	1.01	0.05	5.96	10.0
COM2B-SS1	2	Stiff	0.32	0.40	0.08	2.38	32.6
COM2B-SS2	2	Soft	0.89	0.39	0.08	2.32	3.7
COM3B	4	N/A	0.47	0.66	0.02	3.93	3.2
COM3B-SS1	4	Stiff	0.66	0.23	0.08	1.33	30.1
COM3B-SS2	4	Soft	1.19	0.26	0.06	1.51	5.0

As shown in Figure 6 and Table 5, the lateral strength of the SSI models are much smaller than those of the baseline models. In addition, the ductility of the SSI models is much larger than that of the baseline models. This transfer of strength for ductility is entirely due to a change from the typical braced frame response seen in the baseline models to a response where the braced frames remain essentially elastic while their footings uplift and rock on the soil. Figure 7 compares the deformed shapes of COM2B-SS2 and COM2B at peak lateral displacements from a single response history analysis for an earthquake record scaled to MCE_R. As seen in Figure 7, the braced frame from COM2B undergoes brace deformation and fracture while COM2B-SS2 uplifts pulling the footing away from the soil, while the brace remains essentially elastic.

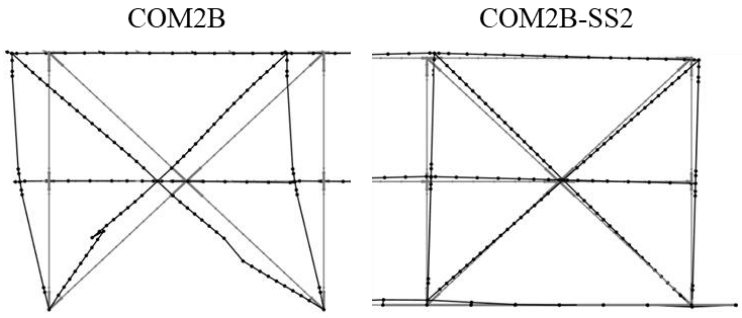

Figure 7 - Comparison of deformed braced frame at peak interstory drift form single MCE_R ground motion

Rocking for the SSI models is expected because of the relatively high over-strength factor. Modern foundation design does not consider over-strength in the structure above the foundation to determine the foundation demand. Instead, an allowable stress design approach for the base shear and overturning moments from ASCE/SEI 7-10 is used for design.

Incremental dynamic analyses (IDAs) were also conducted on all SSI archetype models per the FEMA P-695 methodology using OpenSees. Figure 8 compares the collapse fraction and resulting collapse fragility curves for the SSI models and the corresponding baseline models, in a consistent manner with the data for the baseline models. Table 6 summarizes key values extracted from the IDA plots. These results indicate that the models with SSI have a lower probability of collapse at MCE_R than the models without SSI, but the difference is not extreme because there is a transfer from strength to ductility. The results also show that as the building period decreases, the collapse probability also decreases.

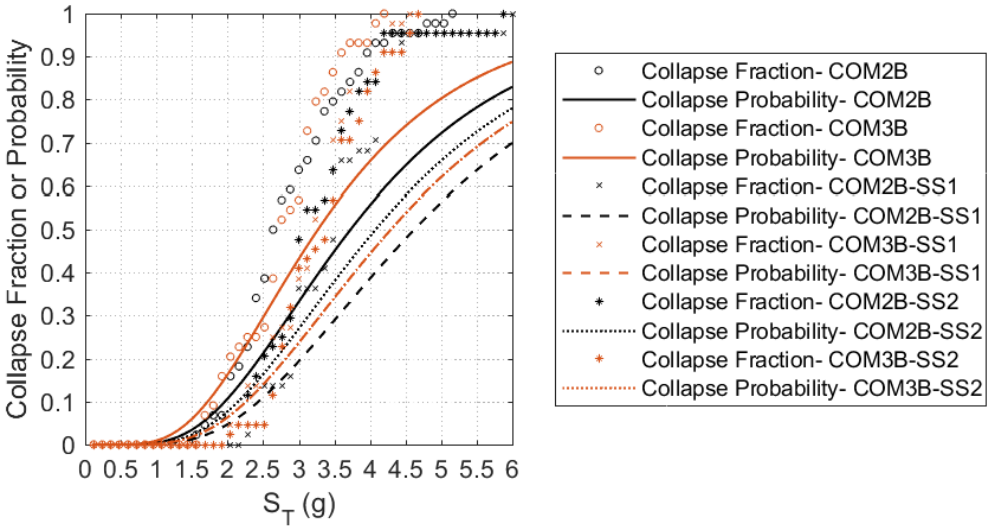

Figure 8 - Collapse fraction and collapse probability curves vs S_T from IDA analyses for the SSI models

Table 6 – Collapse results for SSI models

Archetype ID	No. of Stories	SSI	S_{MT} (g)	S_{CT} (g)	CMR_{3D}	$P[CO\|MCE_R]$
COM2B	2	N/A	1.5	2.34	1.87	3.4%
COM2B-SS1	2	Stiff	1.5	2.90	2.32	1.2%
COM2B-SS2	2	Soft	1.5	2.68	2.15	2.3%
COM3B	4	N/A	1.5	2.29	1.83	6.0%
COM3B-SS1	4	Stiff	1.5	2.65	2.12	1.8%
COM3B-SS2	4	Soft	1.5	2.77	2.22	1.8%

6. Summary and Conclusions

Low-rise commercial buildings with a short period (under 0.5 seconds) are very common in the United States. Previous analytically predicted collapse rates have shown that buildings with a period less than 0.5 seconds have collapse probabilities that increase with decreasing period and may not meet seismic performance objectives. However, these trends have not been observed historically after earthquakes. The gaps between analytically predicted and historically observed collapse rates of short period buildings hints that seismic performance of such buildings is not being accurately predicted by current analytical models.

In this study, A P-695 analysis was completed on a set of archetypes that varied parameters such as number of stories, level of design seismicity, and inclusion of SSI and foundation flexibility. The results of these analyses are in agreement with historical observations after earthquakes: the probability of collapse decreases with decreasing building height for short period buildings. Figure 9 confirms this trend by plotting the probability of collapse verses building period. For archetypes designed for Seismic Design Category D (the circles in the figure) the trend of decreasing collapse probability is clear. Adding SSI and foundation flexibility to those models (denoted by '*' and the boxes) produces a similar, although more muted trend with period. The outliers in Figure 9 are the collapse probabilities for the buildings designed for Seismic Design Category E (shown as an 'x') which are much larger than the other archetypes. This result is due to the low over-strength values for these archetypes as described above. Results for buildings subjected to high seismic ground motions appear to show that the use of improved nonlinear dynamic numerical models can begin to explain the paradox, brining numerical results into closer alignment with observed collapse records.

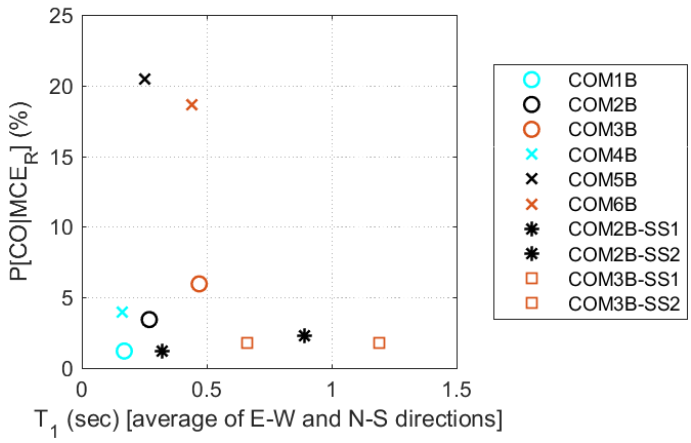

Figure 9 - MCE_R collapse probability verses fundamental period for baseline and SSI models.

7. Acknowledgements

Charles Kircher serves as the Project Technical Director of the FEMA-funded ATC-116 Project and Chair of the Project Technical Committee (PTC). Other key members of the project team include Jeff Berman, Kelly Cobeen, J. Daniel Dolan, Andre Filiatrault, James R. Harris, William T. Holmes, Gregory Kingsley, Larry Kruth, Onder Kustu, Dawn Lehman, Philip Line, Jim Malley, Weichiang Pang, Steve Pryor, Pui-Shum Shing, Lisa Starr and Jason Thompson. Justin Moresco is the ATC Project Manager. Mai (Mike) Tong is the FEMA Task Monitor and Robert D. Hanson is the FEMA Technical Monitor.

The work forming the basis for this publication was conducted pursuant to a contract with the Federal Emergency Management Agency. The substance of such work is dedicated to the public. The authors are solely responsible for the accuracy of statements or interpretations of the ATC-116 Project and the material contained in this article. Opinions, findings, conclusions, or recommendations expressed in this publication do not necessarily reflect the views of the Applied Technology Council (ATC), or the Federal Emergency Management Agency (FEMA). Additionally, neither ATC, FEMA, nor any of their employees, makes any warranty, expressed or implied, nor assumes any legal liability or responsibility for the accuracy,

completeness, or usefulness of any information, product, or process included in this publication.

8. References

References must be cited in the text in square brackets [1, 2], numbered according to the order in which they appear in the text, and listed at the end of the manuscript in a section called References, in the following format:

[1] FEMA (2009): *Quantification of Building Seismic Performance Factors*, FEMA P-695, prepared by the Applied Technology Council for the Federal Emergency Management Agency, Washington, D.C., USA.

[2] NIST (2012): *Tentative Framework for Development of Advanced Seismic Design Criteria for New Buildings, NIST GCR 12-917-20*. National Institute of Standards and Technology, Gaithersburg, MD, USA.

[3] McKenna F, Scott M.H., Fenves G.L (2010): Nonlinear finite-element analysis software architecture using object composition. *Journal of Computing in Civil Engineering*, **24** (1), 95-107.

[4] Hsiao P.C, Lehamn D.E, Roeder C.W (2012): Improved analytical model for special concentrically braced frames. *Journal of Constructional Steel Research*, **73**, 80-94.

[5] Hsiao P.C., Lehamn D.E, Roeder C.W (2013): A model to simulate special concentrically braced frames beyond brace fracture. *Earthquake Engineering & Structural Dynamics*, **42** (2), 183-200.

[6] Sen A.D, Roeder R.W, Lehman D.E, Berman J.W (2019): Nonlinear modeling of concentrically braced frames. *Journal of Constructional Steel Research*, **157**, 103-120.

[7] NIST (2017): *Guidelines for Nonlinear Structural Analysis for Design of Buildings, Part IIa – Steel Moment Frames*, NIST GCR 17-917-46v2. National Institute of Standards and Technology, Gaithersburg, MD, USA.

[8] Lignos D.G, Hartloper, A.R, Elkady, S.M, Deierlein G.G, Hamburger R (2019): Proposed Updates to the ASCE 41 Nonlinear Modeling Parameters for Wide-Flange Steel Columns in Support of Performance-Based Seismic Engineering, *Journal of Structural Engineering*, **145** (9).

